

OmniBind: Large-scale Omni Multimodal Representation via Binding Spaces

Zehan Wang^{1*} Ziang Zhang^{1*} Hang Zhang¹ Luping Liu¹ Rongjie Huang¹
 Xize Cheng¹ Hengshuang Zhao² Zhou Zhao¹
¹Zhejiang University ²The University of HongKong
<http://omnibind.github.io>

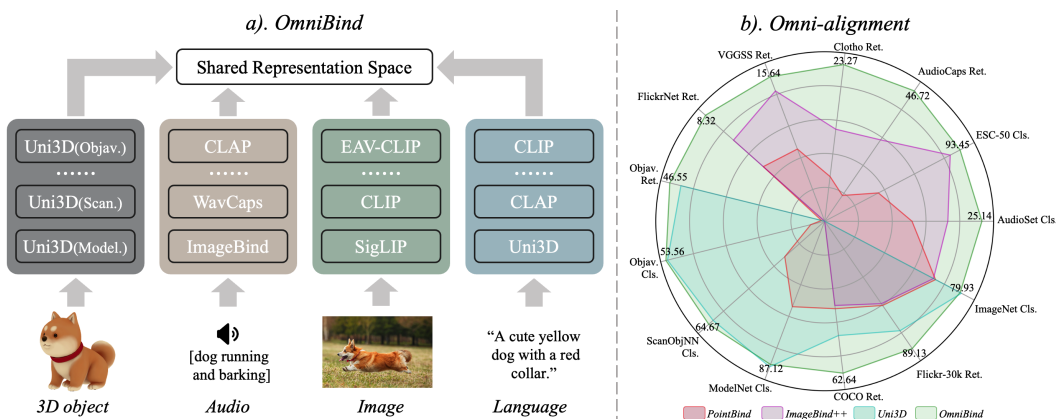


Figure 1: **Overview of OmniBind.** OmniBind integrates diverse knowledge of various existing multimodal models, leading to large-scale omni representations. OmniBind exhibits remarkable versatility and achieves state-of-the-art results on extensive downstream tasks over all modality pairs.

Abstract

Recently, human-computer interaction with various modalities has shown promising applications, like GPT-4o and Gemini. Given the foundational role of multimodal joint representation in understanding and generation pipelines, high-quality omni joint representations would be a step toward co-processing more diverse multimodal information. In this work, we present **OmniBind**, large-scale multimodal joint representation models ranging in scale from 7 billion to 30 billion parameters, which support 3D, audio, image, and language inputs. Due to the scarcity of data pairs across all modalities, instead of training large models from scratch, we propose remapping and binding the spaces of various pre-trained specialist models together. This approach enables "scaling up" by indirectly increasing the model parameters and the amount of seen data. To effectively integrate various spaces, we dynamically assign weights to different spaces by learning routers with two objectives: cross-modal overall alignment and language representation decoupling. Notably, since binding and routing spaces both only require lightweight networks, OmniBind is extremely training-efficient. Learning the largest 30B model requires merely unpaired unimodal data and approximately 3 days on a single 8-4090 node. Extensive experiments demonstrate the versatility and superiority of OmniBind as an omni representation model, highlighting its great potential for diverse applications, such as any-query and composable multimodal understanding.

*Equal contribution. {wangzehan01, ziangzhang}@zju.edu.cn

1 Introduction

Multimodal joint representation, which aligns different modalities into a shared space, forms the foundation of current multimodal understanding [35, 34, 3, 70] and generation pipelines [42, 40, 46, 25]. Recently, co-understanding and generating various modalities with omni model has attracted increasing attention and demonstrates promising application prospects, like GPT-4o [38] and Gemini [50]. However, existing open-source multimodal representation models primarily explore on a relatively small scale and are trained for limited combinations of modalities, such as image-text [41, 66, 48], audio-text [60, 37], audio-image [20, 19] and 3D-image-text [62, 63, 36, 67].

Scaling up achieves incredibly success in language [1, 51, 26, 52] and vision-language models [2, 34, 48]. It consistently improves model performance and generalization by increasing the seen data and model parameters. Therefore, it is appealing to develop a large-scale omni multimodal representation model. However, due to the scarcity of paired data and scalable architectures across every modality, it is difficult to train omni multimodal representation models from scratch.

In this paper, we present **OmniBind**, large-scale unified representation models incorporating 3D, audio, image, and language. Instead of training large models from scratch, we bind numerous spaces together, thereby developing an ensemble model that has indirectly seen massive data and contains a large number of parameters, as shown in Fig. 1-a. By integrating the alignment knowledge between different modalities, the resulting model pieces together omni alignment across all modalities. Moreover, inheriting pre-trained knowledge greatly reduces the computing resources and data requirements. The entire learning process can be completed with several million unpaired data and 4090 GPUs.

However, it is non-trivial to effectively integrate numerous pre-trained spaces. Simply remapping and weighted-averaging spaces as [56], cannot achieve the desired "scaling up". As more spaces are integrated, knowledge from different sources would interfere with each other. Manually adjusting the combining factors only results in trade-offs between different expertise rather than a truly versatile omni model. We attribute the interference and trade-off phenomenon to the fixed combining weight. Spaces trained for different purposes on varied datasets contain knowledge of various aspects, and averaging them with fixed weights can only preserve knowledge of certain aspects.

Inspired by the Mixture-of-Expert technique in LLMs [17, 26, 29, 13], we introduce weights routing strategy to ensemble the spaces, aiming to resolve the above dilemma. Specifically, for each modality, we utilize a learnable router to dynamically predict the combining weights based on input information. Two main objectives guide the training of routers: cross-modal overall alignment and language representation decoupling. The former motivates routers to predict optimal weights for all modality combinations, while the latter is designed to alleviate the conflicts between text embeddings that are aligned to different modalities, and ensure the discrimination of language representations.

With above techniques, we bind 14 existing spaces together, successfully developing three omni models ranging from 7 to 30 billion parameters, named **OmniBind**. Our method showcases impressive performance on extensive multimodal tasks. For 3D, audio, and image classification, OmniBind shows advanced zero-shot generalization ability. It also demonstrates significantly stronger cross-modal alignment on all possible modality pairs. In addition, benefiting from the high-quality omni semantic alignment, OmniBind enables impressive applications, such as accurate 3D-audio retrieval, any-query object localization/audio separation, and complex composable understanding.

Our contributions can be summarized as follows:

- 1) We propose **OmniBind**, large-scale omni multimodal representation models, ranging in scale from 7 billion to 30 billion parameters and encompassing four modalities: 3D point, audio, image, and language. It emphasizes the value of piecing various pre-trained specialist models together.
- 2) We introduce routers to ensemble spaces pre-trained on various modalities and datasets, thereby mitigating interference between knowledge from different sources and further enhancing versatility.
- 3) We design two learning objectives for learning routers: cross-modal overall alignment and language representation decoupling, which motivate routers to dynamically predict the optimal combining weights for all modality pairs while reserving the discrimination of representations.
- 4) OmniBind exhibits state-of-the-art performance on 13 benchmarks that cover all the modality pairs, and great potential for diverse applications, such as 3D-audio retrieval and any-query separation/localization, while requiring minimal computing resources and data.

2 Related Work

2.1 Multimodal Joint Representation

Multimodal joint representation mainly aims to map inputs from different modalities into a shared space. Leveraging the semantic alignment property, pre-trained representation models are widely utilized in current multimodal large language models, such as LLaVA [35, 34], ImageBind-LLM [23], and Chat-3D [55, 24], as well as multimodal generation pipelines like Stable Diffusion [42], SD XL [40], make-a-video [46] and make-an-audio [25].

The initial multimodal representation is CLIP model [41], which demonstrates impressive generalization capabilities in various vision-language downstream tasks. Motivated by its success, successors propose stronger image-language representations by using higher-quality initialization [16, 47], larger-scale datasets [43, 5], improved learning objectives [66], or better model architecture [15, 30]. Besides, some researchers employ the multimodal contrastive learning paradigm in other modality pairs. CLAP [60] and WavCaps [37] learn aligned audio-language space from audio-text pairs.

In addition to these studies improving the alignment of two modalities, another line of work aims to develop unified spaces capable of accommodating inputs from multiple modalities (more than two). For instance, AudioCLIP [22] and WAV2CLIP [59] introduce additional audio encoders for CLIP, leveraging audio-image-text and audio-image pairs. ULIP [62] and Uni3D [67] collect massive amounts of 3D-image-text paired data, enabling them to learn 3D-image-text joint representations based on advanced image-text pre-trained models. More recently, ImageBind [19] and Language-Bind [69] propose to integrate multiple modalities using different data pairs that share the crucial image or language modality.

While current methods showcase a certain degree of robust cross-modal semantic alignment, they are primarily explored at relatively small scales and limited to specific modality pairs. On the other hand, our work focuses on large-scale omni representation models proficient in all modality pairs.

2.2 Scaling Up Models

Scaling up language or vision-language models has been incredibly successful in perception, reasoning, and generation tasks. GPT4 [1] and LLaMA [51, 52] achieve impressive conversation capability via training billion level language models on almost the massive internet language data. Recent InternVL [7] and EVA-CLIP-18B [48] try to scale the parameter of the CLIP model to the ten-billion level. These methods prove that with the growth of model parameters and seen data, models obtain consistent and non-saturating performance improvement.

However, due to the scarcity of paired data across all modalities, the development of large-scale omni multimodal representation models has been lagging. In this paper, we propose to achieve the scaling up by binding existing spaces pre-trained on different modalities and datasets, rather than learning larger models from scratch with more data. This approach results in ensemble models that incorporate diverse knowledge from massive data and range from 7 billion to 30 billion parameters.

2.3 Knowledge Fusion

Fusing knowledge from different sources is a classical and widely-used method to develop robust AI models. Traditional ensemble learning methods [68, 71] train models with different sub-datasets, and combine the output of different models as the final prediction. Similar ideas are also employed by large language model research, recent works [4, 54, 65] propose to merge multiple language models tuned for different downstream tasks, and the resulting model excels at all aspects. Moreover, the Mixture-of-Experts (MoE) language model [17, 26, 8] is also developing a hybrid model consisting of multiple sub-models and obtains better performance or efficiency by integrating them together.

For multimodal representation learning, C-MCR [58] and Ex-MCR [57] first propose to fuse two bi-modality representation space via the shared modality, thereby building unified space with low data and computing resource requirements. FreeBind [56] is a high-level abstract of the above two methods, which employs bi-modality spaces to augment pre-trained unified space. Unlike these methods that only involve a few numbers of spaces, our goal is to obtain large-scale omni representations via binding extensive spaces, which face more severe risks of knowledge interference.

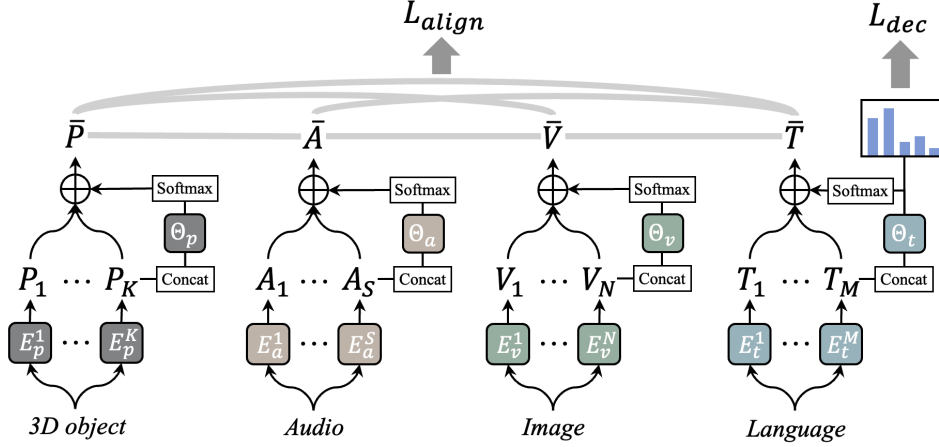


Figure 2: The pipeline of **OmniBind**. The Θ_X denotes the router of modality X , and E_X^i is the i -th encoder of modality X . The losses L_{align} and L_{dec} are the objectives for training the routers.

3 OmniBind

3.1 Spaces Binding

Given that vision-language models are well-resourced and play a pivotal role in the multimodal field, we choose the advanced CLIP model EVA-CLIP-18B [48] as the foundation, and bind additional image-text, audio-text, audio-image-text and 3D-image-text spaces onto it.

For space binding, FreeBind [56] firstly proposes to improve a representation space by integrating extra spaces. Its space binding pipeline can be summarized as two steps: 1) collecting pseudo embedding pairs across two spaces and 2) mapping one space to another. Our binding process is primarily derived from FreeBind, but we replace its pseudo embedding-pair aggregation with a more efficient and robust pseudo item-pair retrieval, and scale up the number of integrated spaces.

Concretely, FreeBind first encodes massive unpaired unimodal data into embeddings of each space, and then uses the cross-modal similarity maps to aggregate pseudo embedding pairs across two spaces. The embedding pairs are unique for each pair of spaces. Therefore, when binding extensive spaces, repeatedly aggregating embeddings would be resource-intensive. Besides, the non-shared pseudo pairs are also unstable due to the varying performance of existing spaces.

To bind spaces robustly and efficiently, we directly retrieve pseudo pairs across all modalities at the item level. Considering lots of unpaired 3D, audio, image, and language data, and leveraging the most advanced 3D-image-text, audio-text, audio-image, and image-text retrieval model, we can take each modality as a starting point to retrieve the top-1 recall of data from other modalities. This approach constructs the pseudo item pairs $\{p, a, v, t\}$.

Using the pseudo data, we train simple projectors to individually bind each space to EVA-CLIP-18B. The training objective of the projector is the multimodal contrastive loss between all pairs of involved modalities. For instance, when binding CLAP with EVA-CLIP-18B, the learning objective is:

$$L_{bind} = \text{Info}(\Psi(\mathbf{A}_{at}), \mathbf{T}_{vt}) + \text{Info}(\Psi(\mathbf{A}_{at}), \mathbf{V}_{vt}) + \text{Info}(\Psi(\mathbf{T}_{at}), \mathbf{T}_{vt}) + \text{Info}(\Psi(\mathbf{T}_{at}), \mathbf{V}_{vt}) \quad (1)$$

where \mathbf{A}_{at} , \mathbf{T}_{at} are CLAP embeddings, \mathbf{V}_{vt} , \mathbf{T}_{vt} are EVA-CLIP-18B embeddings and the $\Psi(\cdot)$ is a multi-layer perceptron projector. The $\text{Info}(\cdot, \cdot)$ is multimodal contrastive loss:

$$\text{Info}(\mathbf{X}, \mathbf{Y}) = -\frac{1}{2} \sum_{i=1}^B \left(\log \frac{e^{(\mathbf{x}_i \cdot \mathbf{y}_i) / \tau}}{\sum_{j=1}^N e^{(\mathbf{x}_i \cdot \mathbf{y}_j) / \tau}} + \log \frac{e^{(\mathbf{y}_i \cdot \mathbf{x}_i) / \tau}}{\sum_{j=1}^N e^{(\mathbf{y}_i \cdot \mathbf{x}_j) / \tau}} \right) \quad (2)$$

Binding all different spaces together results in a hybrid model with K 3D point encoders, S audio encoders, N image encoders, and M text encoders. These encoders originate from different pre-trained models but share the same encoding space after binding. The representations of the resulting ensemble model can be calculated as:

$$\bar{\mathbf{P}} = \sum_{i=1}^K \alpha_i \cdot \mathbf{P}_i; \quad \bar{\mathbf{A}} = \sum_{i=1}^S \beta_i \cdot \mathbf{A}_i; \quad \bar{\mathbf{V}} = \sum_{i=1}^N \gamma_i \cdot \mathbf{V}_i; \quad \bar{\mathbf{T}} = \sum_{i=1}^M \delta_i \cdot \mathbf{T}_i; \quad (3)$$

where the $\bar{\mathbf{P}}, \bar{\mathbf{A}}, \bar{\mathbf{V}}, \bar{\mathbf{T}}$ are the embeddings of resulting model, and $\mathbf{P}_i, \mathbf{A}_i, \mathbf{V}_i, \mathbf{T}_i$ respectively denote the 3D point, audio, image, and text representations from each corresponding i -th encoder. The $\alpha_i, \beta_i, \gamma_i, \delta_i$ are the combining factors for i -th encoder of each modality.

3.2 Weights Routing

Existing works [58, 57, 56] manually set the combining factors of encoders from different spaces. While manual settings offer flexibility to customize the resulting space when integrating a few spaces, it is increasingly complex and impractical as more spaces are added. Moreover, hand-designed combining weights also limit the deep integration across various knowledge sources, leading to simple trade-offs rather than comprehensive incorporation of different expertise.

To address this issue, drawing inspiration from the Mixture-of-Expert (MoE) technique in Large Language Models (LLMs), we propose dynamically assigning weights with learnable routers. As shown in Fig. 2, each modality contains one router to predict the corresponding combining factors for encoders of this modality, which can be formulated as:

$$\begin{aligned} \alpha_1, \dots, \alpha_K &= \text{softmax}(\Theta_p(\mathbf{P})); \beta_1, \dots, \beta_S = \text{softmax}(\Theta_a(\mathbf{A})) \\ \gamma_1, \dots, \gamma_N &= \text{softmax}(\Theta_v(\mathbf{V})); \delta_1, \dots, \delta_M = \text{softmax}(\Theta_t(\mathbf{T})) \end{aligned} \quad (4)$$

where $\mathbf{P}, \mathbf{A}, \mathbf{V}, \mathbf{T}$ are the concatenated outputs of each modality, and the $\Theta_p, \Theta_a, \Theta_v, \Theta_t$ denote the router for 3D point, audio, image and language, respectively. To develop effective and robust routers, we utilize the entire retrieved pseudo dataset $\{p, a, v, t\}$ and design two learning objectives:

Cross-modal Overall Alignment. To motivate routers to predict the optimal weights for all modality combinations, we employ contrastive losses overall modality pairs as the first learning target:

$$L_{align} = \text{Info}(\bar{\mathbf{A}}, \bar{\mathbf{P}}) + \text{Info}(\bar{\mathbf{A}}, \bar{\mathbf{V}}) + \text{Info}(\bar{\mathbf{A}}, \bar{\mathbf{T}}) + \text{Info}(\bar{\mathbf{P}}, \bar{\mathbf{V}}) + \text{Info}(\bar{\mathbf{P}}, \bar{\mathbf{T}}) + \text{Info}(\bar{\mathbf{V}}, \bar{\mathbf{T}}) \quad (5)$$

where $\bar{\mathbf{P}}, \bar{\mathbf{A}}, \bar{\mathbf{V}}, \bar{\mathbf{T}}$ are defined in Eq. 3. By simply averaging the contrastive losses between all modality pairs, we cultivate balanced routers that achieve comprehensively high-quality cross-modal semantic alignment over all modalities.

Language Representation Decoupling. Compared to 3D points, audio, and images, which are primarily sampled from the real world, language data is entirely artificial, exhibiting much higher information density and a stronger ideographic tendency. Therefore, textual descriptions of different modalities exhibit significant biases: image captions often describe appearances, audio captions focus on sounding actions, and 3D captions prioritize spatial structures. As a result, text encoders trained to align different modalities demonstrate more specialized expertise than encoders of other modalities.

Considering the significant distribution variance among the different text representations, we introduce an auxiliary learning objective for the language router to disentangle the language representation and improve its generalization. It preserves the discrimination of text embedding space and enhances the semantic alignments with various modalities. Specifically, we drive the language router to identify which modality the input texts are likely describing and to prioritize text encoders that are specialized in the corresponding modality. To this end, we define the loss function as follows:

$$L_{dec} = - \sum_{j=1}^M [y_j \log(\Theta_t(\mathbf{T})_j) + (1 - y_j) \log(1 - \Theta_t(\mathbf{T})_j)] \quad (6)$$

where the M is the number of text encoders. The texts in the retrieved pseudo-paired dataset are collected from audio-text, image-text, and 3D-text pairs. Correspondingly, the text encoders are also derived from models pre-trained for audio-text, image-text, and 3D-text alignment. In Eq. 6, $y_j = 1$ if the input text and the j -th text encoder are related to the same modality and $y_j = 0$ otherwise.

Finally, we linearly combine the above two objectives, and the final loss can be expressed as:

$$L = \lambda L_{dec} + L_{align} \quad (7)$$

3.3 Model Configurations

The projectors Ψ used for aligning spaces are simple two-layer MLPs. Additionally, we employ the mixture-of-projectors strategy following [56]. The routers Θ are similarly designed as two-layer MLPs, with an extra sigmoid activation function at the end.

We select 14 pre-trained spaces for binding, which can be grouped into five audio-text (three WavCaps [37], two LIANO-CLAPs [60]), five image-text (EVA-CLIP-18B [48], EVA02-CLIP-E [15] two SigLIPs [66], DFN-ViT-H [14]), three 3D-image-text (three Uni3Ds [67]) and one audio-image-text (ImageBind [19]) spaces. After binding all spaces to EVA-CLIP-18B, we construct three configurations of OmniBind by combining different spaces: **OmniBind-Base**, **OmniBind-Large**, and **OmniBind-Full** with 7 billion, 13 billion and 30 billion parameters. The encoder parameters for each modality and the specific spaces used in each variant are detailed in Appendix B.

4 Experiment

4.1 Implementation

Datasets & Hyper-parameter. To construct the pseudo-paired data, we collect unpaired 3D point, audio, image, and text data from the training set of existing datasets. For 3D data, we use the 800k 3D point clouds from Objaverse [9]. The audio and image data come from AudioSet [18] and ImageNet [10] respectively. The text data sources from three kinds of datasets: 3D-text [36], visual-text [33, 45] and audio-text [27, 12] datasets. Based on these unpaired unimodal data, we employ state-of-the-art audio-text (WavCaps [37]), image-text (EVA-CLIP-18B [48]), audio-image (ImageBind [19]) and 3D-image-text (Uni3D [67]) models to retrieve the pseudo item pairs, as discussed in Sec. 3.1. The temperature factors in contrastive losses are 0.03, and the λ in Eq. 7 is 3.

Benchmarks & Baselines. To comprehensively access the performance of our omni representations, we conduct quantitative experiments across 13 benchmarks covering 7 downstream tasks, as summarized in Tab. 1. In these benchmarks, we compare OmniBinds with three groups of previous multimodal representation models: 1) 3D-image-text models: Uni3D’s pre-trained and three fine-tuned variants [67]. 2) audio-image-text models: C-MCR [58], LanguageBind [69], ImageBind [19], ImageBind++ [56] and InternVL_{IB++} [56]. 3) 3D-audio-image-text models: Ex-MCR [57] and PointBind [21]. Moreover, we provide the best results on each benchmark achieved by the 14 source specialist spaces for reference, denoted as "Individual Best".

Table 1: Statistic for evaluation tasks and benchmarks.

Task	Modality	Benchmarks	Items
Zero-shot Classification	Audio	AudioSet [18]	19,048
		ESC-50 [39]	400
	Image	ImageNet-1K [10]	50,000
	3D	Objaverse-LVIS [9]	46,832
ScanObjNN [53]		2,890	
ModelNet40 [61]		2,468	
Cross-modal Retrieval	Audio-Text	AudioCaps [27]	964
		Clotho [12]	1,045
	Audio-Image	VGG-SS [6]	5,158
		FlickrNet [44]	5,000
	Image-Text	COCO [33]	5,000
		Flickr-30K [64]	1,000
3D-Image	Objaverse-LVIS [9]	46,205	

4.2 Performance Results

Cross-modal Retrieval. As aforementioned, OmniBind aims to provide high-quality semantic alignment between all modality pairs. Therefore, we comprehensively assess the cross-modal retrieval performance across all possible modality pairs. The quantitative results for audio-text, audio-image, image-text, and 3D-image retrieval are presented in Tab. 2.

Overall, OmniBind-Full and OmniBind-Large consistently outperform all previous methods across all benchmarks. Some prior approaches demonstrate competitive performance within their specific domains. For instance, ImageBind++ shows similarly strong audio-image alignment, and InternVL_{IB++} displays comparable image-text capabilities, but they both fall short in other areas and lack support for 3D input. Compared to existing 3D-audio-image-text models like Ex-MCR and PointBind, all OmniBind variants exhibit substantial and comprehensive advantages across all combinations of modalities. These observations underscore the versatility and superiority of OmniBind.

Moreover, OmniBind-Full achieves similar performance to the "Individual Best", demonstrating that OmniBind successfully inherits and effectively integrates the expertise of various source spaces. Remarkably, OmniBind achieves even better audio-image and 3D-image alignment, showcasing the exciting cross-space knowledge transfer. By incorporating the high-quality image representations learned from image-text data, the audio-image and 3D-image alignment can also be improved.

Table 2: Cross-modal retrieval results. Best result is **bolded**, and second best result is underlined.

Models	Audio-Text				Audio-Image				Image-Text				3D-Image	
	AudioCaps		Clotho		VGG-SS		FlickrNet		COCO		Flickr30K		Objaverse	
	R@1	R@5	R@1	R@5	R@1	R@5	R@1	R@5	R@1	R@5	R@1	R@5	R@1	R@5
Uni3D	×	×	×	×	×	×	×	×	59.51	81.45	87.85	97.55	43.57	67.61
C-MCR	15.76	41.37	8.37	24.86	1.94	7.69	1.39	5.97	16.67	37.04	34.16	63.64	×	×
LanguageBind	12.42	36.70	11.32	31.03	2.55	9.86	1.52	6.36	53.24	76.48	82.36	96.19	×	×
ImageBind	9.24	27.47	6.64	17.28	14.82	35.67	7.68	20.79	57.28	79.54	86.04	96.97	×	×
ImageBind++	29.16	62.98	13.67	33.19	<u>15.48</u>	39.26	<u>8.01</u>	<u>21.87</u>	57.01	79.23	85.91	97.03	×	×
InternVL _{IB} ++	29.11	62.30	12.66	32.75	14.40	36.78	7.74	21.85	<u>61.07</u>	<u>82.00</u>	89.30	98.09	×	×
Ex-MCR	19.07	47.05	7.01	22.04	2.13	8.13	1.57	5.94	40.24	64.78	71.89	90.55	2.54	8.25
PointBind	9.24	27.47	6.64	17.28	14.82	35.67	7.68	20.79	57.28	79.54	86.04	96.97	5.86	14.59
OmniBind-Base	43.61	76.02	20.94	46.77	14.11	35.74	7.67	21.65	56.94	80.11	85.99	97.02	34.34	58.40
OmniBind-Large	47.89	79.75	<u>23.07</u>	49.67	14.14	36.07	7.86	21.72	60.08	82.35	87.20	97.40	<u>46.09</u>	<u>69.11</u>
OmniBind-Full	<u>46.72</u>	<u>79.69</u>	23.27	<u>49.46</u>	15.64	<u>38.19</u>	8.32	23.49	62.64	83.79	<u>89.13</u>	<u>97.82</u>	46.55	69.92
Individual Best	48.22	81.15	23.57	49.13	14.82	35.67	7.68	20.79	63.69	84.09	90.83	98.33	43.57	67.61

Table 3: Zero-shot classification results. Uni3D, Uni3D(Objav.), Uni3D(Scan.) and Uni3D(Model.) represent the pre-trained and three fine-tuned version of Uni3D-g, respectively.

Model	Audio			Image		3D					
	AudioSet	ESC-50		ImageNet		Objaverse		ScanObjectNN		ModelNet40	
	mAP	Top1	Top5	Top1	Top5	Top1	Top5	Top1	Top5	Top1	Top5
Uni3D	×	×	×	80.12	95.97	53.13	81.59	64.12	91.63	87.56	99.27
Uni3D(Objav.)	×	×	×	80.12	95.97	54.74	82.54	58.89	88.69	84.20	98.42
Uni3D(Scan.)	×	×	×	80.12	95.97	50.99	80.00	65.81	92.70	<u>88.05</u>	98.58
Uni3D(Model.)	×	×	×	<u>80.12</u>	<u>95.97</u>	51.21	80.14	64.43	90.66	88.05	<u>99.11</u>
C-MCR	11.15	70.35	96.70	24.50	52.44	×	×	×	×	×	×
LanguageBind	18.33	94.00	99.70	77.15	94.64	×	×	×	×	×	×
ImageBind	13.96	67.25	87.50	76.31	94.23	×	×	×	×	×	×
ImageBind++	19.69	90.30	99.30	76.01	94.36	×	×	×	×	×	×
InternVL _{IB} ++	18.93	87.75	98.75	81.21	96.68	×	×	×	×	×	×
Ex-MCR	6.67	71.20	96.80	60.79	86.98	17.94	43.37	40.31	77.20	66.53	93.60
PointBind	13.96	67.25	87.50	76.13	94.22	13.83	30.34	55.05	86.89	76.18	97.04
OmniBind-Base	21.19	92.90	99.75	76.18	94.02	53.30	81.85	57.79	89.76	82.82	97.12
OmniBind-Large	25.57	93.25	<u>99.80</u>	78.87	95.32	<u>53.97</u>	<u>82.90</u>	64.67	<u>94.15</u>	86.55	99.03
OmniBind-Full	<u>25.14</u>	<u>93.45</u>	99.85	79.93	95.86	53.56	81.82	<u>64.67</u>	94.36	87.12	99.03
Individual Best	23.36	94.05	99.75	82.43	96.73	54.74	82.54	65.81	92.70	88.05	99.11

Zero-shot Classification. To further validate the generalization ability of OmniBind, we conduct zero-shot classification on each modality, and report the results in Tab. 3.

For audio and image classification, OmniBind demonstrates overall superiority, even when compared to models excelling in the audio-image-text domains. While LanguageBind performs slightly better than OmniBind on ESC-50, all variants of OmniBind significantly outperform previous methods on the more challenging AudioSet benchmark. This highlights the robustness and generalization of OmniBind. Furthermore, although InternVL_{IB}++ achieves the highest accuracy on ImageNet, it falls short in audio classification, which further showcases the versatility of OmniBind.

In 3D object classification, the three fine-tuned variants of Uni3D perform exceptionally well on their respective fine-tuned datasets. OmniBind-Base, which leverages only Uni3D(Objav.) as the 3D-image-text source space, achieves performance comparable to Uni3D(Objav.), demonstrating that the binding space effectively inherits knowledge from the source space. Additionally, OmniBind-Large and OmniBind-Full integrate the knowledge from all three fine-tuned versions, performing well across various benchmarks and exhibiting the best overall performance.



Figure 3: Qualitative comparison of audio to 3D object retrieval. More visualizations of 3D-audio retrieval are provided in the Appendix C.

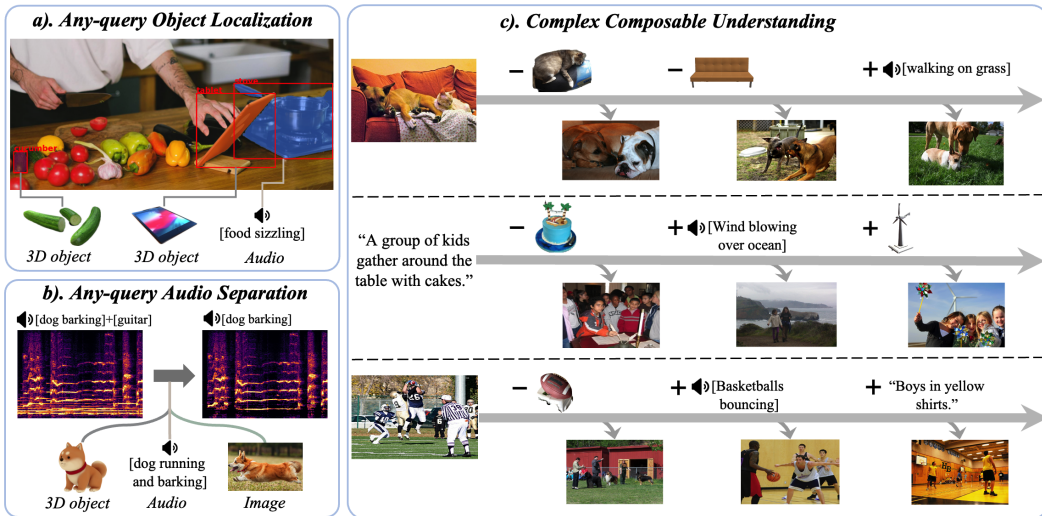


Figure 4: Diverse applications enabled by OmniBind.

4.3 Applications

Emergent cross-modal alignment. OmniBind reveals a surprising emergent alignment between 3D and audio. In Fig. 3 and 6, we randomly sample audios from AudioCaps and retrieve relevant 3D objects in Objaverse. OmniBind shows a deep understanding of each modality and high-quality semantic alignment. For example, it accurately recognizes the audio of "cat purring" and "violin" and finds the corresponding 3D models. In the "clock ticktock" case, while PointBind and Ex-MCR struggle to distinguish disk-shaped 3D models, OmniBind successfully identifies mechanical clocks.

Any-query object localization. OmniBind also demonstrates high-quality fine-grain semantic alignment, enabling any-query object localization. By extracting object proposals using pre-trained object segmentation [28] models, we can match these object proposals with queries from any modality within OmniBind’s space. As shown in Fig. 4-a, we can localize objects in images using sounds or 3D models as queries.

Any-query audio separation. We replace the CLIP embeddings in CLIPSep [11] with OmniBind and fine-tune it on our pseudo dataset. In Fig. 4-b, we observe that we can successfully separate audios of a dog barking using queries from images, audio, language, and even 3D models of a dog.

Complex composable understanding. Impressively, OmniBind’s embedding space not only enables addition and subtraction between arbitrary embeddings but also supports complex serial embedding arithmetic. Three representative cases are provided in Fig. 4-c. In the first case, starting with a photo of "one cat and one dog on sofa," we sequentially subtract the embeddings of a 3D cat and a 3D sofa to obtain "two dogs on sofa" and "two dogs not on sofa." Adding the sound of walking on grass then results in "two dogs on the grass." Similar exciting capabilities are observed in two other examples.

Table 4: Ablation study of manual weights and the two weight routing objectives: L_{align} and L_{dec} . *AT high*, *VT high*, and *PVT high* indicate manually assigning higher weights to audio-text, image-text, and 3D-image-text spaces, respectively. *Mean* means averaging all spaces. The Top1 and R@1 metrics of 3D classification and cross-modal retrieval are reported. The dataset names are abbreviated.

Setting	L_{align}	L_{dec}	3D classification			Audio-Text		Audio-Image		Image-Text		3D-Image
			Objav.	Scan.	Model.	ACaps	Clotho	VGGSS	FNet	COCO	F30K	Objav.
<i>AT high</i>	-	-	49.47	59.90	85.17	44.47	21.76	14.33	7.69	55.97	84.81	46.23
<i>VT high</i>	-	-	53.44	64.19	86.99	33.24	17.49	13.82	7.45	61.38	<u>88.57</u>	46.24
<i>PVT high</i>	-	-	53.35	63.08	87.07	34.95	18.08	13.18	7.34	59.86	87.84	48.18
<i>Mean</i>	-	-	52.29	62.46	86.47	40.31	20.33	13.40	7.35	59.61	87.61	44.61
Weight Routing	×	✓	53.70	64.81	87.40	48.48	24.31	13.93	7.35	<u>61.86</u>	88.27	44.61
	✓	×	52.93	63.98	85.74	43.71	20.44	<u>15.62</u>	8.35	59.43	87.64	<u>46.73</u>
	✓	✓	<u>53.56</u>	<u>64.67</u>	<u>87.12</u>	<u>46.72</u>	<u>23.27</u>	15.64	<u>8.32</u>	62.64	89.13	46.55

More potentials. Previous multimodal joint representations [67, 19, 69] enable other applications, like point cloud painting [67], any-to-any generation [49], and omnimulti modal LLMs [23, 32]. Given that OmniBind is essentially homologous to the representation models used in previous applications and contains more diverse and generalizable knowledge, it holds great potential for these applications as well. We leave these explorations for future work.

4.4 Ablation Study

Performance improvement with more spaces. The integrated spaces and parameters of our three variants: OmniBind-Base, OmniBind-Large, and OmniBind-Full, sequentially increase. From Tab. 2 and 3, we observe consistent overall performance improvements with the growth of the model scale, further proving the effectiveness of "scaling up" representations model via binding more spaces.

Trade-offs in manually assigned weights. Tab. 4 shows the performance of four types of manually assigned weights: *AT high*, *VT high*, *PVT high* and *Mean*. These four variants reveal trade-off phenomena among different areas of expertise. *AT high* performs well in the audio-text domain but is less effective in 3D classification and image-text tasks. Conversely, *VT high* (*PVT high*) obtains better image-text (3D-image) performance at the expense of audio-text alignment. *Mean* exhibits a more balanced performance but lacks specific expertise. Moreover, using weight routing showcases a comprehensive advantage over these manual weight variants. This observation further proves the routers can effectively alleviate interference between knowledge of different sources, leading to overall improvements in performance rather than simple trade-offs.

Effectiveness of L_{align} & L_{dec} for learning routers. We provide the ablation experiments for the two learning objectives in Tab. 4. By comparing the *Mean* and variants using each objective separately, we conclude that L_{align} brings noticeable improvements across all possible modality combinations, while L_{dec} specifically and significantly enhances language-related alignment. Combining the two objectives yields the best overall performance by complementing each other's strengths.

Improved discrimination with L_{dec} . To explore the effect of language representation decoupling on discrimination, we extract language embeddings from all AudioCaps and COCO captions. We find that employing L_{dec} reduces the cosine similarity between all the possible language embedding pairs from 0.0828 to 0.0517. As discussed in [31], lower cosine similarity between irrelevant pairs indicates the embeddings "occupy" more space in the hypersphere. Therefore, employing L_{dec} indeed enhances the discrimination of language representations, leading to better overall performance.

5 Conclusion

In this work, we present OmniBind, large-scale omni multimodal representation models ranging in scale from 7 billion to 30 billion parameters. Our core contributions include successfully scaling up multimodal representation by binding many existing spaces and designing a weight routing strategy to mitigate interference between knowledge of different sources. By combining 14 pre-trained spaces, OmniBind demonstrates impressive multimodal performance across extensive benchmarks and shows vast potential for further growth and diverse applications.

References

- [1] Josh Achiam, Steven Adler, Sandhini Agarwal, Lama Ahmad, Ilge Akkaya, Florencia Leoni Aleman, Diogo Almeida, Janko Altenschmidt, Sam Altman, Shyamal Anadkat, et al. Gpt-4 technical report. *arXiv preprint arXiv:2303.08774*, 2023.
- [2] Jean-Baptiste Alayrac, Jeff Donahue, Pauline Luc, Antoine Miech, Iain Barr, Yana Hasson, Karel Lenc, Arthur Mensch, Katherine Millican, Malcolm Reynolds, et al. Flamingo: a visual language model for few-shot learning. *Advances in neural information processing systems*, 35:23716–23736, 2022.
- [3] Jinze Bai, Shuai Bai, Shusheng Yang, Shijie Wang, Sinan Tan, Peng Wang, Junyang Lin, Chang Zhou, and Jingren Zhou. Qwen-vl: A frontier large vision-language model with versatile abilities. *arXiv preprint arXiv:2308.12966*, 2023.
- [4] Rachit Bansal, Bidisha Samanta, Siddharth Dalmia, Nitish Gupta, Shikhar Vashishth, Sriram Ganapathy, Abhishek Bapna, Prateek Jain, and Partha Talukdar. Llm augmented llms: Expanding capabilities through composition. *arXiv preprint arXiv:2401.02412*, 2024.
- [5] Minwoo Byeon, Beomhee Park, Haecheon Kim, Sungjun Lee, Woonhyuk Baek, and Sae-hoon Kim. Coyo-700m: Image-text pair dataset. <https://github.com/kakaobrain/coyo-dataset>, 2022.
- [6] Honglie Chen, Weidi Xie, Triantafyllos Afouras, Arsha Nagrani, Andrea Vedaldi, and Andrew Zisserman. Localizing visual sounds the hard way. In *Proceedings of the IEEE/CVF conference on computer vision and pattern recognition*, pages 16867–16876, 2021.
- [7] Zhe Chen, Jiannan Wu, Wenhai Wang, Weijie Su, Guo Chen, Sen Xing, Zhong Muyan, Qinglong Zhang, Xizhou Zhu, Lewei Lu, et al. Internvl: Scaling up vision foundation models and aligning for generic visual-linguistic tasks. *arXiv preprint arXiv:2312.14238*, 2023.
- [8] Aakanksha Chowdhery, Sharan Narang, Jacob Devlin, Maarten Bosma, Gaurav Mishra, Adam Roberts, Paul Barham, Hyung Won Chung, Charles Sutton, Sebastian Gehrmann, et al. Palm: Scaling language modeling with pathways. *Journal of Machine Learning Research*, 24(240):1–113, 2023.
- [9] Matt Deitke, Dustin Schwenk, Jordi Salvador, Luca Weihs, Oscar Michel, Eli VanderBilt, Ludwig Schmidt, Kiana Ehsani, Aniruddha Kembhavi, and Ali Farhadi. Objaverse: A universe of annotated 3d objects. In *Proceedings of the IEEE/CVF Conference on Computer Vision and Pattern Recognition*, pages 13142–13153, 2023.
- [10] Jia Deng, Wei Dong, Richard Socher, Li-Jia Li, Kai Li, and Li Fei-Fei. Imagenet: A large-scale hierarchical image database. In *2009 IEEE conference on computer vision and pattern recognition*, pages 248–255. Ieee, 2009.
- [11] Hao-Wen Dong, Naoya Takahashi, Yuki Mitsufuji, Julian McAuley, and Taylor Berg-Kirkpatrick. Clipsep: Learning text-queried sound separation with noisy unlabeled videos. *arXiv preprint arXiv:2212.07065*, 2022.
- [12] Konstantinos Drossos, Samuel Lipping, and Tuomas Virtanen. Clotho: An audio captioning dataset. In *ICASSP 2020-2020 IEEE International Conference on Acoustics, Speech and Signal Processing (ICASSP)*, pages 736–740. IEEE, 2020.
- [13] Nan Du, Yanping Huang, Andrew M Dai, Simon Tong, Dmitry Lepikhin, Yuanzhong Xu, Maxim Krikun, Yanqi Zhou, Adams Wei Yu, Orhan Firat, et al. Glam: Efficient scaling of language models with mixture-of-experts. In *International Conference on Machine Learning*, pages 5547–5569. PMLR, 2022.
- [14] Alex Fang, Albin Madappally Jose, Amit Jain, Ludwig Schmidt, Alexander Toshev, and Vaishaal Shankar. Data filtering networks. *arXiv preprint arXiv:2309.17425*, 2023.
- [15] Yuxin Fang, Quan Sun, Xinggang Wang, Tiejun Huang, Xinlong Wang, and Yue Cao. Eva-02: A visual representation for neon genesis. *arXiv preprint arXiv:2303.11331*, 2023.

- [16] Yuxin Fang, Wen Wang, Binhui Xie, Quan Sun, Ledell Wu, Xinggang Wang, Tiejun Huang, Xinlong Wang, and Yue Cao. Eva: Exploring the limits of masked visual representation learning at scale. In *Proceedings of the IEEE/CVF Conference on Computer Vision and Pattern Recognition*, pages 19358–19369, 2023.
- [17] William Fedus, Barret Zoph, and Noam Shazeer. Switch transformers: Scaling to trillion parameter models with simple and efficient sparsity. *Journal of Machine Learning Research*, 23(120):1–39, 2022.
- [18] Jort F Gemmeke, Daniel PW Ellis, Dylan Freedman, Aren Jansen, Wade Lawrence, R Channing Moore, Manoj Plakal, and Marvin Ritter. Audio set: An ontology and human-labeled dataset for audio events. In *2017 IEEE international conference on acoustics, speech and signal processing (ICASSP)*, pages 776–780. IEEE, 2017.
- [19] Rohit Girdhar, Alaaeldin El-Nouby, Zhuang Liu, Mannat Singh, Kalyan Vasudev Alwala, Armand Joulin, and Ishan Misra. Imagebind: One embedding space to bind them all. In *Proceedings of the IEEE/CVF Conference on Computer Vision and Pattern Recognition*, pages 15180–15190, 2023.
- [20] Yuan Gong, Andrew Rouditchenko, Alexander H Liu, David Harwath, Leonid Karlinsky, Hilde Kuehne, and James Glass. Contrastive audio-visual masked autoencoder. *arXiv preprint arXiv:2210.07839*, 2022.
- [21] Ziyu Guo, Renrui Zhang, Xiangyang Zhu, Yiwen Tang, Xianzheng Ma, Jiaming Han, Kexin Chen, Peng Gao, Xianzhi Li, Hongsheng Li, et al. Point-bind & point-llm: Aligning point cloud with multi-modality for 3d understanding, generation, and instruction following. *arXiv preprint arXiv:2309.00615*, 2023.
- [22] Andrey Guzhov, Federico Raue, Jörn Hees, and Andreas Dengel. Audioclip: Extending clip to image, text and audio. In *ICASSP 2022-2022 IEEE International Conference on Acoustics, Speech and Signal Processing (ICASSP)*, pages 976–980. IEEE, 2022.
- [23] Jiaming Han, Renrui Zhang, Wenqi Shao, Peng Gao, Peng Xu, Han Xiao, Kaipeng Zhang, Chris Liu, Song Wen, Ziyu Guo, et al. Imagebind-llm: Multi-modality instruction tuning. *arXiv preprint arXiv:2309.03905*, 2023.
- [24] Haifeng Huang, Zehan Wang, Rongjie Huang, Luping Liu, Xize Cheng, Yang Zhao, Tao Jin, and Zhou Zhao. Chat-3d v2: Bridging 3d scene and large language models with object identifiers. *arXiv preprint arXiv:2312.08168*, 2023.
- [25] Rongjie Huang, Jiawei Huang, Dongchao Yang, Yi Ren, Luping Liu, Mingze Li, Zhenhui Ye, Jinglin Liu, Xiang Yin, and Zhou Zhao. Make-an-audio: Text-to-audio generation with prompt-enhanced diffusion models. In *International Conference on Machine Learning*, pages 13916–13932. PMLR, 2023.
- [26] Albert Q Jiang, Alexandre Sablayrolles, Antoine Roux, Arthur Mensch, Blanche Savary, Chris Bamford, Devendra Singh Chaplot, Diego de las Casas, Emma Bou Hanna, Florian Bressand, et al. Mixtral of experts. *arXiv preprint arXiv:2401.04088*, 2024.
- [27] Chris Dongjoo Kim, Byeongchang Kim, Hyunmin Lee, and Gunhee Kim. Audiocaps: Generating captions for audios in the wild. In *Proceedings of the 2019 Conference of the North American Chapter of the Association for Computational Linguistics: Human Language Technologies, Volume 1 (Long and Short Papers)*, pages 119–132, 2019.
- [28] Alexander Kirillov, Eric Mintun, Nikhila Ravi, Hanzi Mao, Chloe Rolland, Laura Gustafson, Tete Xiao, Spencer Whitehead, Alexander C Berg, Wan-Yen Lo, et al. Segment anything. In *Proceedings of the IEEE/CVF International Conference on Computer Vision*, pages 4015–4026, 2023.
- [29] Dmitry Lepikhin, HyoukJoong Lee, Yuanzhong Xu, Dehao Chen, Orhan Firat, Yanping Huang, Maxim Krikun, Noam Shazeer, and Zhifeng Chen. Gshard: Scaling giant models with conditional computation and automatic sharding. *arXiv preprint arXiv:2006.16668*, 2020.

- [30] Yanghao Li, Haoqi Fan, Ronghang Hu, Christoph Feichtenhofer, and Kaiming He. Scaling language-image pre-training via masking. In *Proceedings of the IEEE/CVF Conference on Computer Vision and Pattern Recognition*, pages 23390–23400, 2023.
- [31] Victor Weixin Liang, Yuhui Zhang, Yongchan Kwon, Serena Yeung, and James Y Zou. Mind the gap: Understanding the modality gap in multi-modal contrastive representation learning. *Advances in Neural Information Processing Systems*, 35:17612–17625, 2022.
- [32] Bin Lin, Bin Zhu, Yang Ye, Munan Ning, Peng Jin, and Li Yuan. Video-llava: Learning united visual representation by alignment before projection. *arXiv preprint arXiv:2311.10122*, 2023.
- [33] Tsung-Yi Lin, Michael Maire, Serge Belongie, James Hays, Pietro Perona, Deva Ramanan, Piotr Dollár, and C Lawrence Zitnick. Microsoft coco: Common objects in context. In *Computer Vision–ECCV 2014: 13th European Conference, Zurich, Switzerland, September 6-12, 2014, Proceedings, Part V 13*, pages 740–755. Springer, 2014.
- [34] Haotian Liu, Chunyuan Li, Yuheng Li, and Yong Jae Lee. Improved baselines with visual instruction tuning. *arXiv preprint arXiv:2310.03744*, 2023.
- [35] Haotian Liu, Chunyuan Li, Qingyang Wu, and Yong Jae Lee. Visual instruction tuning. *Advances in neural information processing systems*, 36, 2024.
- [36] Minghua Liu, Ruoxi Shi, Kaiming Kuang, Yinhao Zhu, Xuanlin Li, Shizhong Han, Hong Cai, Fatih Porikli, and Hao Su. Openshape: Scaling up 3d shape representation towards open-world understanding. *Advances in Neural Information Processing Systems*, 36, 2024.
- [37] Xinhao Mei, Chutong Meng, Haohe Liu, Qiuqiang Kong, Tom Ko, Chengqi Zhao, Mark D Plumbley, Yuexian Zou, and Wenwu Wang. Wavcaps: A chatgpt-assisted weakly-labelled audio captioning dataset for audio-language multimodal research. *arXiv preprint arXiv:2303.17395*, 2023.
- [38] OpenAI. Gpt-4o. <https://openai.com/index/hello-gpt-4o/>, 2024.
- [39] Karol J Piczak. Esc: Dataset for environmental sound classification. In *Proceedings of the 23rd ACM international conference on Multimedia*, pages 1015–1018, 2015.
- [40] Dustin Podell, Zion English, Kyle Lacey, Andreas Blattmann, Tim Dockhorn, Jonas Müller, Joe Penna, and Robin Rombach. Sdxl: Improving latent diffusion models for high-resolution image synthesis. *arXiv preprint arXiv:2307.01952*, 2023.
- [41] Alec Radford, Jong Wook Kim, Chris Hallacy, Aditya Ramesh, Gabriel Goh, Sandhini Agarwal, Girish Sastry, Amanda Askell, Pamela Mishkin, Jack Clark, et al. Learning transferable visual models from natural language supervision. In *International conference on machine learning*, pages 8748–8763. PMLR, 2021.
- [42] Robin Rombach, Andreas Blattmann, Dominik Lorenz, Patrick Esser, and Björn Ommer. High-resolution image synthesis with latent diffusion models. In *Proceedings of the IEEE/CVF conference on computer vision and pattern recognition*, pages 10684–10695, 2022.
- [43] Christoph Schuhmann, Romain Beaumont, Richard Vencu, Cade Gordon, Ross Wightman, Mehdi Cherti, Theo Coombes, Aarush Katta, Clayton Mullis, Mitchell Wortsman, et al. Laion-5b: An open large-scale dataset for training next generation image-text models. *Advances in Neural Information Processing Systems*, 35:25278–25294, 2022.
- [44] Arda Senocak, Tae-Hyun Oh, Junsik Kim, Ming-Hsuan Yang, and In So Kweon. Learning to localize sound source in visual scenes. In *Proceedings of the IEEE Conference on Computer Vision and Pattern Recognition*, pages 4358–4366, 2018.
- [45] Piyush Sharma, Nan Ding, Sebastian Goodman, and Radu Soricut. Conceptual captions: A cleaned, hypernymed, image alt-text dataset for automatic image captioning. In *Proceedings of the 56th Annual Meeting of the Association for Computational Linguistics (Volume 1: Long Papers)*, pages 2556–2565, 2018.

- [46] Uriel Singer, Adam Polyak, Thomas Hayes, Xi Yin, Jie An, Songyang Zhang, Qiyuan Hu, Harry Yang, Oron Ashual, Oran Gafni, et al. Make-a-video: Text-to-video generation without text-video data. *arXiv preprint arXiv:2209.14792*, 2022.
- [47] Quan Sun, Yuxin Fang, Ledell Wu, Xinlong Wang, and Yue Cao. Eva-clip: Improved training techniques for clip at scale. *arXiv preprint arXiv:2303.15389*, 2023.
- [48] Quan Sun, Jinsheng Wang, Qiyang Yu, Yufeng Cui, Fan Zhang, Xiaosong Zhang, and Xinlong Wang. Eva-clip-18b: Scaling clip to 18 billion parameters. *arXiv preprint arXiv:2402.04252*, 2024.
- [49] Zineng Tang, Ziyi Yang, Chenguang Zhu, Michael Zeng, and Mohit Bansal. Any-to-any generation via composable diffusion. *Advances in Neural Information Processing Systems*, 36, 2024.
- [50] Gemini Team, Rohan Anil, Sebastian Borgeaud, Yonghui Wu, Jean-Baptiste Alayrac, Jiahui Yu, Radu Soricut, Johan Schalkwyk, Andrew M Dai, Anja Hauth, et al. Gemini: a family of highly capable multimodal models. *arXiv preprint arXiv:2312.11805*, 2023.
- [51] Hugo Touvron, Thibaut Lavril, Gautier Izacard, Xavier Martinet, Marie-Anne Lachaux, Timothée Lacroix, Baptiste Rozière, Naman Goyal, Eric Hambro, Faisal Azhar, et al. Llama: Open and efficient foundation language models. *arXiv preprint arXiv:2302.13971*, 2023.
- [52] Hugo Touvron, Louis Martin, Kevin Stone, Peter Albert, Amjad Almahairi, Yasmine Babaei, Nikolay Bashlykov, Soumya Batra, Prajjwal Bhargava, Shruti Bhosale, et al. Llama 2: Open foundation and fine-tuned chat models. *arXiv preprint arXiv:2307.09288*, 2023.
- [53] Mikaela Angelina Uy, Quang-Hieu Pham, Binh-Son Hua, Thanh Nguyen, and Sai-Kit Yeung. Revisiting point cloud classification: A new benchmark dataset and classification model on real-world data. In *Proceedings of the IEEE/CVF international conference on computer vision*, pages 1588–1597, 2019.
- [54] Fanqi Wan, Xinting Huang, Deng Cai, Xiaojun Quan, Wei Bi, and Shuming Shi. Knowledge fusion of large language models. *arXiv preprint arXiv:2401.10491*, 2024.
- [55] Zehan Wang, Haifeng Huang, Yang Zhao, Ziang Zhang, and Zhou Zhao. Chat-3d: Data-efficiently tuning large language model for universal dialogue of 3d scenes. *arXiv preprint arXiv:2308.08769*, 2023.
- [56] Zehan Wang, Ziang Zhang, Xize Cheng, Rongjie Huang, Luping Liu, Zhenhui Ye, Haifeng Huang, Yang Zhao, Tao Jin, Peng Gao, and Zhou Zhao. Freebind: Free lunch in unified multimodal space via knowledge fusion. *arXiv preprint arXiv:2405.04883*, 2024.
- [57] Zehan Wang, Ziang Zhang, Luping Liu, Yang Zhao, Haifeng Huang, Tao Jin, and Zhou Zhao. Extending multi-modal contrastive representations. *arXiv preprint arXiv:2310.08884*, 2023.
- [58] Zehan Wang, Yang Zhao, Haifeng Huang, Jiageng Liu, Aoxiong Yin, Li Tang, Linjun Li, Yongqi Wang, Ziang Zhang, and Zhou Zhao. Connecting multi-modal contrastive representations. *Advances in Neural Information Processing Systems*, 36:22099–22114, 2023.
- [59] Ho-Hsiang Wu, Prem Seetharaman, Kundan Kumar, and Juan Pablo Bello. Wav2clip: Learning robust audio representations from clip. In *ICASSP 2022-2022 IEEE International Conference on Acoustics, Speech and Signal Processing (ICASSP)*, pages 4563–4567. IEEE, 2022.
- [60] Yusong Wu*, Ke Chen*, Tianyu Zhang*, Yuchen Hui*, Taylor Berg-Kirkpatrick, and Shlomo Dubnov. Large-scale contrastive language-audio pretraining with feature fusion and keyword-to-caption augmentation. In *IEEE International Conference on Acoustics, Speech and Signal Processing, ICASSP*, 2023.
- [61] Zhirong Wu, Shuran Song, Aditya Khosla, Fisher Yu, Linguang Zhang, Xiaoou Tang, and Jianxiong Xiao. 3d shapenets: A deep representation for volumetric shapes. In *Proceedings of the IEEE conference on computer vision and pattern recognition*, pages 1912–1920, 2015.

- [62] Le Xue, Mingfei Gao, Chen Xing, Roberto Martín-Martín, Jiajun Wu, Caiming Xiong, Ran Xu, Juan Carlos Niebles, and Silvio Savarese. Ulip: Learning a unified representation of language, images, and point clouds for 3d understanding. In *Proceedings of the IEEE/CVF Conference on Computer Vision and Pattern Recognition*, pages 1179–1189, 2023.
- [63] Le Xue, Ning Yu, Shu Zhang, Artemis Panagopoulou, Junnan Li, Roberto Martín-Martín, Jiajun Wu, Caiming Xiong, Ran Xu, Juan Carlos Niebles, et al. Ulip-2: Towards scalable multimodal pre-training for 3d understanding. *arXiv preprint arXiv:2305.08275*, 2023.
- [64] Peter Young, Alice Lai, Micah Hodosh, and Julia Hockenmaier. From image descriptions to visual denotations: New similarity metrics for semantic inference over event descriptions. *Transactions of the Association for Computational Linguistics*, 2:67–78, 2014.
- [65] Le Yu, Bowen Yu, Haiyang Yu, Fei Huang, and Yongbin Li. Language models are super mario: Absorbing abilities from homologous models as a free lunch. *arXiv preprint arXiv:2311.03099*, 2023.
- [66] Xiaohua Zhai, Basil Mustafa, Alexander Kolesnikov, and Lucas Beyer. Sigmoid loss for language image pre-training. In *Proceedings of the IEEE/CVF International Conference on Computer Vision*, pages 11975–11986, 2023.
- [67] Junsheng Zhou, Jinsheng Wang, Baorui Ma, Yu-Shen Liu, Tiejun Huang, and Xinlong Wang. Uni3d: Exploring unified 3d representation at scale. *arXiv preprint arXiv:2310.06773*, 2023.
- [68] Zhi-Hua Zhou and Zhi-Hua Zhou. *Ensemble learning*. Springer, 2021.
- [69] Bin Zhu, Bin Lin, Munan Ning, Yang Yan, Jiayi Cui, HongFa Wang, Yatian Pang, Wenhao Jiang, Junwu Zhang, Zongwei Li, et al. Languagebind: Extending video-language pretraining to n-modality by language-based semantic alignment. *arXiv preprint arXiv:2310.01852*, 2023.
- [70] Deyao Zhu, Jun Chen, Xiaoqian Shen, Xiang Li, and Mohamed Elhoseiny. Minigt-4: Enhancing vision-language understanding with advanced large language models. *arXiv preprint arXiv:2304.10592*, 2023.
- [71] Mohammad Zounemat-Kermani, Okke Batelaan, Marzieh Fadaee, and Reinhard Hinkelmann. Ensemble machine learning paradigms in hydrology: A review. *Journal of Hydrology*, 598:126266, 2021.

A Limitations and Future Works

Although OmniBind is already the largest multimodal representation model, demonstrating remarkable versatility and generalization, it currently utilizes only 14 existing spaces and 4 modalities: 3D, audio, images, and text. It remains to be explored whether or when this binding space-based "scaling up" will reach saturation. Additionally, this work only presents three basic applications as inspiration. Investigating whether using higher-quality and larger-scale omni multimodal representations can enable new capabilities in downstream applications would be a promising direction.

B Statistics of OmniBind Variants

The detailed source spaces used to build OmniBind-Base, OmniBind-Large, and OmniBind-Full are presented in Tables 5, 6, and 7, respectively. Generally speaking, OmniBind-Base comprises three components: three WavCaps, EVA02-CLIP-E, Uni3D (Objaverse), and ImageBind. The primary difference between OmniBind-Large and OmniBind-Full is the inclusion of EVA-CLIP-18B in OmniBind-Full. Additionally, we provide statistics on the number of parameters for OmniBind-Base, OmniBind-Large, and OmniBind-Full in Table 8.

Table 5: Source spaces for building OmniBind-Base.

OmniBind-Base	
Audio-Text	WavCaps [37], WavCaps (Clotho) [37], WavCaps (AudioCaps) [37]
Image-Text	EVA02-CLIP-E [15]
3D-Image-Text	Uni3D (Objav.) [67]
Audio-Image-Text	ImageBind [19]

Table 6: Source spaces for building OmniBind-Large.

OmniBind-Large	
Audio-Text	WavCaps [37], WavCaps (Clotho) [37], WavCaps (AudioCaps) [37], LAION-CLAP (general) [60], LAION-CLAP (music) [60]
Image-Text	EVA02-CLIP-E [15], DFN-ViT-H [14], SigLIP-Large [66], SigLIP-so400M [66]
3D-Image-Text	Uni3D (Objav.) [67], Uni3D (Scan.) [67], Uni3D (Model.) [67]
Audio-Image-Text	ImageBind [19]

Table 7: Source spaces for building OmniBind-Full.

OmniBind-Full	
Audio-Text	WavCaps [37], WavCaps (Clotho) [37], WavCaps (AudioCaps) [37], LAION-CLAP (general) [60], LAION-CLAP (music) [60]
Image-Text	EVA-CLIP-18B [48], EVA02-CLIP-E [15] DFN-ViT-H [14], SigLIP-Large [66], SigLIP-so400M [66]
3D-Image-Text	Uni3D (Objav.) [67], Uni3D (Scan.) [67], Uni3D (Model.) [67]
Audio-Image-Text	ImageBind [19]

C More Visualizations

To further qualitatively assess the capabilities of OmniBind, we provide additional visualizations. Each sample is manually evaluated and categorized: correct samples are marked in green, incorrect ones in red, and partially correct ones in orange.

Table 8: Statistics about parameter number of three OmniBind variants.

Variants	Parameter Number					Total
	3D Encoder	Audio Encoder	Image Encoder	Text Encoder	Projector	
OmniBind-Base	1.0B	99M	4.6B	1.3B	224M	7.2B
OmniBind-Large	3.0B	329M	6.0B	2.5B	431M	12.3B
OmniBind-Full	3.0B	329M	23.6B	3.2B	431M	30.6B

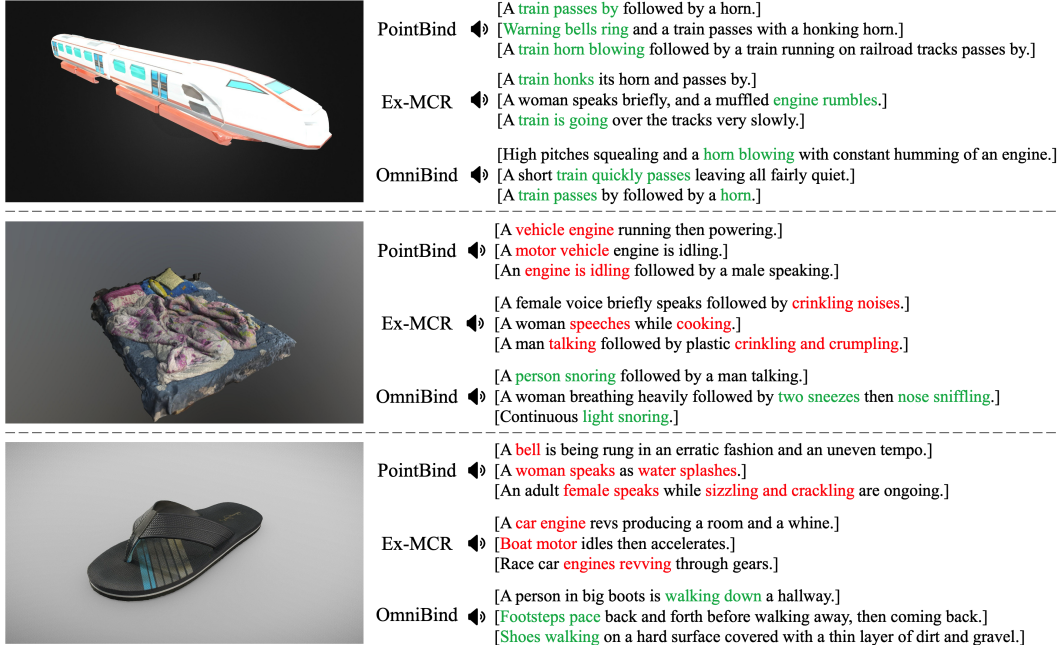


Figure 5: More visualization of 3D-to-Audio retrieval.

In Fig. 5, we randomly select three 3D objects from Objaverse and retrieve relevant audio clips from AudioCaps. The captions for the retrieved audio clips are provided. OmniBind demonstrates more accurate retrieval results compared to previous methods (PointBind and Ex-MCR).

Furthermore, we present additional cases of audio to 3D object retrieval in Figs. 6. In each instance, the 3D objects retrieved by OmniBind exhibit significantly better semantic alignment with the audio query than those retrieved by Ex-MCR and PointBind.

D Social Impact

OmniBind is a method for learning large-scale multimodal representation models by aligning and reorganizing knowledge from existing pre-trained models. Therefore, the capability of OmniBind is mainly inherited from the source pre-trained models. Implementing additional safety detection and filtering processes for these pre-trained models can effectively reduce the potential for misuse and mitigate negative social impacts of OmniBind.

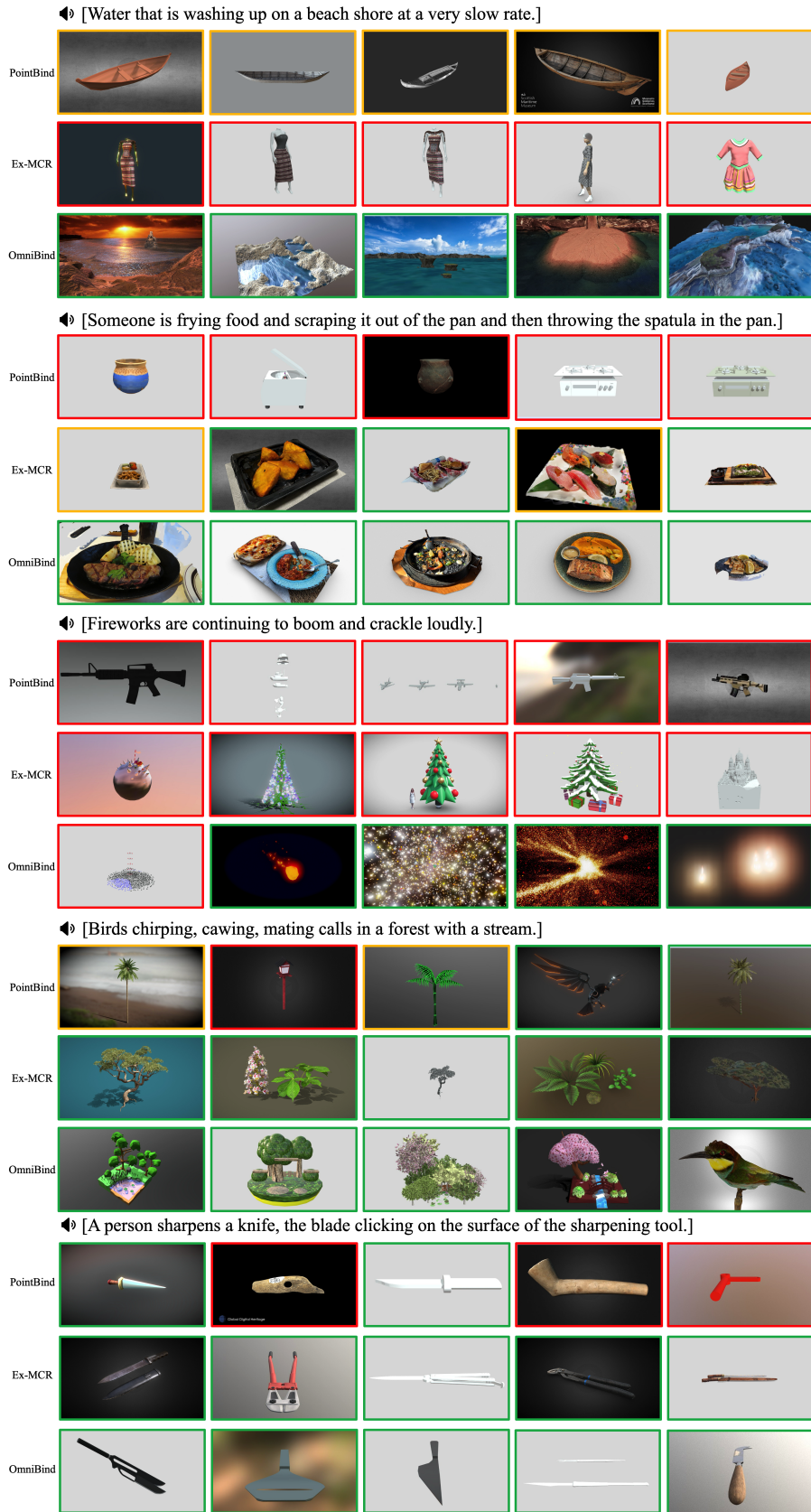


Figure 6: More visualization of Audio-to-3D retrieval.